Phase behaviour of a fluid in slit-like pores with differently adsorbing walls: application of a density functional approach



2002 J. Phys.: Condens. Matter 14 165

(http://iopscience.iop.org/0953-8984/14/2/304)

INSTITUTE OF PHYSICS PUBLISHING JOURNAL OF PHYSICS: CONDENSED MATTER

J. Phys.: Condens. Matter **14** (2002) 165–172 PII: S0953-8984(02)29152-3

# Phase behaviour of a fluid in slit-like pores with differently adsorbing walls: application of a density functional approach

**Roman Zagórski**[1], **Andrzej Patrykiejew and Stefan Sokołowski**

Department for the Modelling of Physico-Chemical Processes, Maria Curie–Skłodowska University, 20031 Lublin, Poland

Received 20 September 2001
Published 13 December 2001
Online at stacks.iop.org/JPhysCM/14/165

**Abstract**

We study the adsorption of a Lennard-Jones gas in a slit-like pore formed by two walls exhibiting different adsorbing properties. The calculations are carried out by means of a density functional approach. We show that changes in the potential field exerted by one wall can lead to substantial modifications in the phase behaviour of confined fluids.

## 1. Introduction

If a fluid is confined to a porous adsorbent, its phase behaviour significantly differs from that of a relevant bulk fluid under identical thermodynamic conditions. The effects of fluid confinement on phase transitions have been studied for a long time, cf the review papers [1–4]. One of the most often explored models was the model of a slit-like pore. Usually, both pore walls have been assumed to be formed by two identical, energetically homogeneous and geometrically flat surfaces. Recently, investigations into adsorption in slit-like pores with energetically heterogeneous walls have also been carried out, demonstrating the significance of heterogeneity effects on the phase behaviour of a confined fluid.

Two surfaces forming a slit do not need to be identical; in fact they can exhibit different adsorbing properties. In the literature there are several papers [5–13] concerning the phase behaviour of ferromagnetic Ising films and binary mixtures (and polymers) confined to slit-like pores with the walls exerting opposing surface fields (so-called 'competing walls'). In such a case a novel type of phase transition can be observed. This transition occurs from a state with an interface fluctuating perpendicularly to the pore walls to a state where the interface is parallel to the walls and is called localization–delocalization transition. It has been demonstrated that for film thicknesses approaching infinity, the transition critical temperature does not converge towards the bulk critical temperature, $T_c$, but rather towards the wetting

[1] Current address: Department of Elektrotechnology, Faculty of Materials Science, Metallurgy and Transport, Silesian University of Technology, 40-019 Katowice, Poland.

0953-8984/02/020165+08$30.00  

transition temperature. As the wetting transition can be either second or first order, the interface localization–delocalization transition can also be second or first order. In addition, it was found [6, 7] that when the wetting transition is first order, the novel transition may be second order for sufficiently thin films.

Identical walls and 'competing walls' are two extreme cases. Thus it is interesting to study how the phase diagram of a confined fluid is altered when the adsorbing potential due to one pore wall is systematically weakened from the initial value, common for both walls, to zero. Such studies have been carried out for a lattice gas confined to a slit-like pore with differently adsorbing walls quite recently [14]. We have observed that if the adsorption energy due to one wall becomes weaker and weaker, a single coexistence envelope, which describes capillary condensation in a pore with two identical walls, splits into several, layering-like branches. The goal of this note is to check if a similar behaviour can also be found for lattice-off systems. The tool we use for that purpose is a density functional approach. Although a non-perturbative density functional approach has recently been proposed [15] we still apply here the standard method, developed by Tarazona [16] according to which the excess Helmholtz free energy is divided into the reference hard sphere and the attractive parts.

## 2. Theory

Let us formulate the model first. We assume that the pore walls are energetically homogeneous, that is the potential exerted by a single wall, $v^{(i)}(z)$, is a function of the normal distance, $z$, only. The external field due to both pore walls is given by

$$v(z) = v^{(1)}(z) + v^{(2)}(H - z) \tag{1}$$

where $H$ is the pore width. In general, the functions $v^{(i)}$ describing the interactions of fluid particles with the first ($v^{(1)}$) and with the second wall ($v^{(2)}(z)$) are different. We model these two functions using the Lennard-Jones (9, 3) potential

$$v^{(i)}(x) = \begin{cases} \varepsilon_i[(z_0/x)^9 - (z_0/x)^3] & x > 0 \\ \infty & \text{otherwise} \end{cases} \tag{2}$$

$i = 1, 2$. In some cases the function $v^{(2)}(H - z)$ is given by a hard-wall (HW) potential

$$v^{(2)}(x) = \begin{cases} 0 & x > 0 \\ \infty & \text{otherwise.} \end{cases} \tag{3}$$

The fluid particles interact via the truncated Lennard-Jones potential

$$u(r) = \begin{cases} \varepsilon[(\sigma/r)^{12} - (\sigma/r)^6] & r < r_{\text{cut}} \\ 0 & \text{otherwise} \end{cases} \tag{4}$$

where $r_{\text{cut}}$ is the cut-off distance, and $\sigma$ is the Lennard-Jones diameter. We assumed $r_{\text{cut}} = 2.5\sigma$ and $z_0 = 0.5\sigma$. Hereafter we use $\sigma$ and $\varepsilon$ as the units of length and energy, respectively. We also define the reduced temperature as $T^* = kT/\varepsilon$. The grand potential functional $\Omega[\rho]$ is expressed as

$$\Omega[\rho] = F[\rho] + \int \{v(z; H) - \mu\}\rho(z)\,\mathrm{d}\boldsymbol{r} \tag{5}$$

where $F[\rho]$ and $\mu$ are the configurational free energy and the configurational chemical potential of the fluid, respectively and $\rho(z)$ is the local density. The equilibrium value of $\Omega$ is obtained minimizing the functional, at a constant temperature, chemical potential and the pore width.

The free-energy functional $F[\rho]$ consists of two parts: an ideal gas part, $F^{\mathrm{id}}$, and an excess part, $F^{\mathrm{ex}}$. The ideal contribution has the form $F^{\mathrm{id}}/kT = \int \rho(z)[\ln \rho(z) - 1]\,\mathrm{d}\boldsymbol{r}$, whereas the excess Helmholtz free energy is divided into the reference hard-sphere contributions $F^{\mathrm{ex}} = F^{\mathrm{ex,hs}} + F^{\mathrm{ex,att}}$. We used the Tarazona approach [16] to evaluate the excess-free-energy functional for hard spheres. Thus

$$F^{\mathrm{ex,hs}}[\rho] = \int \rho(z) f^{\mathrm{hs}}[\tilde{\rho}(z)]\,\mathrm{d}\boldsymbol{r} \tag{6}$$

where $f^{\mathrm{hs}}$ denotes the free energy per particle, resulting from the Carnahan–Starling equation of state and $\tilde{\rho}(z)$ is the weighted density. The attractive energy contribution to the free-energy functional is determined by invoking a mean-field approximation, thus

$$F^{\mathrm{ex,att}} = \tfrac{1}{2} \iint \rho(z)\rho(z')u_a(|\boldsymbol{r} - \boldsymbol{r}'|)\,\mathrm{d}\boldsymbol{r}\,\mathrm{d}\boldsymbol{r}' \tag{7}$$

where the division of the Lennard-Jones potential (4), into attractive and repulsive parts has been performed according to the recipe of Weeks, Chandler and Andersen [17].

The amount of confined fluid equals

$$\Gamma = \int \rho(z)\,\mathrm{d}z \tag{8}$$

and the density profile equation, obtained from the condition $\delta\Omega/\delta\rho(z) = 0$ reads

$$\mu = kT \ln \rho(z) + v(z; H) + f^{\mathrm{hs}}[\tilde{\rho}(z)] + \int \rho(z') \frac{\delta f^{\mathrm{hs}}[\tilde{\rho}(z')]}{\delta\rho(z)}\,\mathrm{d}z' + \int \rho(z')u_a\big(|\boldsymbol{r} - \boldsymbol{r}'|\big)\,\mathrm{d}\boldsymbol{r}'. \tag{9}$$

The configurational chemical potential of a bulk fluid of density $\rho_{\mathrm{b}}$ is $\mu = kT \ln \rho_{\mathrm{b}} + f^{\mathrm{hs}}(\rho_{\mathrm{b}}) + \rho_{\mathrm{b}}[\partial f^{\mathrm{hs}}(\rho_{\mathrm{b}})/\partial\rho_{\mathrm{b}}] + \rho_{\mathrm{b}} \int u_a(r)\,\mathrm{d}\boldsymbol{r}$.

## 3. Results and discussion

In order to demonstrate how the difference in the adsorbing properties of two pore walls influences the phase diagram of a confined fluid, we have performed calculations for several pores characterized by a fixed value of the parameter $\varepsilon_1 = 9.5$ (in units of $\varepsilon$) and various values of $\varepsilon_2$. The parameter $\varepsilon_1$ is rather low; we simply want to avoid the appearance of layering transitions in the case of a pore with identical walls. Our calculations have been preceded by the study of wettability of a single wall, characterized by the same value of the parameter $\varepsilon_1$. In this case we found a first-order wetting and the prewetting transition. The value of the reduced wetting temperature is $T_{\mathrm{w}}^* \simeq 0.805$, whereas the estimated value of the reduced surface critical temperature is approximately equal to 0.93. Note that the bulk critical temperature, obtained from the bulk counterpart of the theory equals $T_{\mathrm{c}}^* = 1.325$. The results for a single adsorbing wall are summarized in figure 1, where a part of the phase diagram with the prewetting line is displayed. We stress that no layering transitions within the investigated interval of the temperatures, $T^* > 0.69$, have been found for this system.

We now return to the behaviour of the confined fluid. Figure 2 shows a series of phase diagrams obtained for the pores with width $H = 10$ and characterized by different values of the parameters $\varepsilon_2 = 9.5, 4.75, 3.8, 2.85, 1.9, 0.95, 0.475$. We also show the phase diagram obtained for the pore with one HW. The phase diagrams were evaluated in an usual way i.e. from the dependences of $\Omega$ on $\mu$, cf [18]. Obviously, when $\varepsilon_2 = 9.5$, we deal with a slit-like pore formed between identical walls. In this case the confinement of the fluid leads to the usual capillary condensation phenomenon, i.e. the entire phase diagram shifts down along the temperature

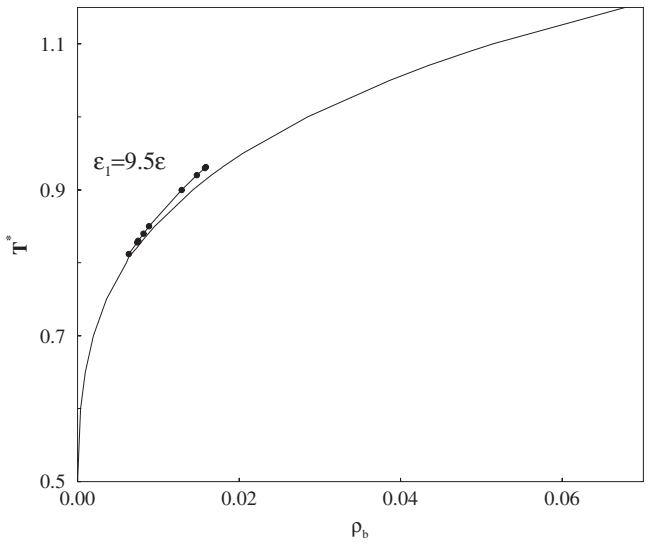


**Figure 1.** The gas–liquid part of the bulk phase diagram (solid curve). Dotted curve shows prewetting line for adsorption on a single wall with $\varepsilon_1 = 9.5$.

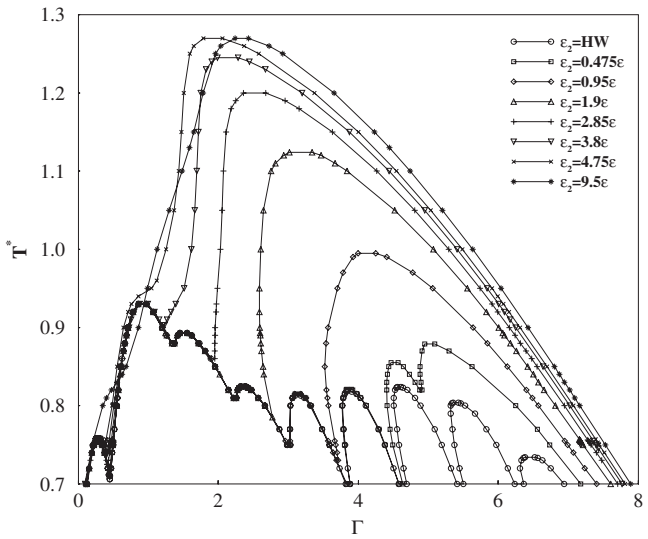


**Figure 2.** Phase diagrams for Lennard-Jones fluid confined to slit-like pores with width $H = 10$, $\varepsilon_1 = 9.5$ and different values of $\varepsilon_2$, listed in the figure. HW means that the second wall is just a HW.

axis with respect to the bulk-phase diagram. The reduced critical capillary condensation temperature equals to $T^*_{cc} = 1.27$ and the value of the average density (averaged over the entire pore), $\langle\rho\rangle = \Gamma/H$, at the critical capillary condensation point is 0.234. The capillary condensation envelope is asymmetric. In particular, the change in wettability of the pore walls at $T^* \gtrsim 0.8$ causes development of a 'knee' at low values of $\Gamma$.

If the attractive potential exerted by the second wall is decreased to, $\varepsilon_2 \approx 4.9$ (the relevant curve is not presented in figure 2), the qualitative picture of the system phase behaviour does

not change. The critical temperature of the capillary condensation is almost identical as in the pore with identical walls. However, the knee observed for $\varepsilon_2 = 9.5$ gently transforms into two steps. A similar situation persists up to $\varepsilon_2 \simeq 4.85$. However, for still lower values of $\varepsilon_2$ the phase diagrams splits into two branches, separated by the triple points, cf the curve evaluated for $\varepsilon_2 = 4.75$. The fist branch (i.e. the branch at low values of $\Gamma$) is markedly smaller than the second one, which reflects the 'specific' capillary condensation.

A consecutive decrease in the value of $\varepsilon_2$ is accompanied by further modifications of the phase diagram. For $\varepsilon_2 = 3.8$ we observe the existence of three branches, whereas for $\varepsilon_2 = 2.85$ the coexistence line is composed of four branches, separated by triple points. For $\varepsilon_2 = 0.95$ the number of branches is six. Each of the branches is characterized by its own critical temperature. However, the development of a new branch at a given value of $\varepsilon_2$ only slightly influences the branches developed at higher values of $\varepsilon_2$. The maximum number of branches (nine) is formed when the second pore wall is just a HW. We also realize a decrease in the triple point temperatures between higher-number branches; in the case when the second wall is a HW, the triple point temperature is between a fifth and a sixth and additionally the consecutive triple point temperature becomes less than 0.7. As at temperatures lower than the bulk triple temperature the reliability of the density functional theory may be questioned, we did not perform the relevant calculations at temperatures less than 0.7.

Figure 3(a) shows an example of the adsorption isotherm at $T^* = 0.8$, and figure 3(b) the density profiles at the same temperature, evaluated for the pore $H = 10$ with $\varepsilon_2 = 0.475$. Consecutive steps in the adsorption correspond to the consecutive branches of the phase diagram (at that temperature there are four transitions in the system). The density profiles in figure 3(b) show equilibrium fluid structures before and after relevant phase transition. For $\varepsilon_2 = 0.475$ the attractive force due to the second pore wall is very small and the space adjacent to this wall remains almost empty. The first adsorption step in figure 3(a) resembles the prewetting step on a single wall, cf the density profiles shown in figure 3(b). However, the temperature at which this transition takes place is slightly lower than the wetting temperature. Similar behaviour of the adsorption isotherm in the pore has been also found at still lower temperatures, $T_w^* > T^* > T_{t,4}^*$, where $T_{t,4}^* \simeq 0.745$ is the fourth triple point temperature. Steps 2 and 3 in the isotherm displayed in figure 3(a) are layering types. However, the layered structure (cf figure 3(b)) is poorly developed. We recall that no layering transitions have been found for a single wall. Finally, step 4 corresponds to the final pore filling, but after this transition the second adsorbing wall remains still dry.

A question appears about the character of the transition corresponding to the first, small branch of the phase diagram in figure 2. This transition takes place for $\varepsilon_2 \lesssim 4.85$ and its critical temperature is approximately equal to 0.75. The insets in figures 3(a) and (b) show respectively the adsorption isotherm jump and the equilibrium density profiles before and after this transition, evaluated for the same system as the isotherm and the profiles in the main parts of these figures, but at $T^* = 0.73$. The jump in the adsorption isotherm is very low and the local densities indicate that this transition takes place within the first layer adjacent to the first pore wall.

Figure 4 illustrates the influence of the pore width on the shape of the phase diagrams. There are plotted coexistence envelopes for three pore widths, $H = 8$, 10 and 12. For each pore we have plotted the diagrams evaluated for the second wall interacting via the Lennard-Jones (9, 3) potential with $\varepsilon_2 = 9.5$ (i.e. for pores with two identical walls), $\varepsilon_2 = 1.9$ and for pores with the second wall being just a HW. It is interesting that in the case of the pores with non-identical walls, the initial parts of the diagrams coincide almost ideally. For example, comparing the diagrams for the pore with $\varepsilon_2 = 1.9$, the first three branches are almost identical for the pores with widths $H = 8$, 10 and 12. Also, a part of the fourth branch is almost identical for the pores with widths $H = 10$ and 12. This is particularly well seen for the pores with the

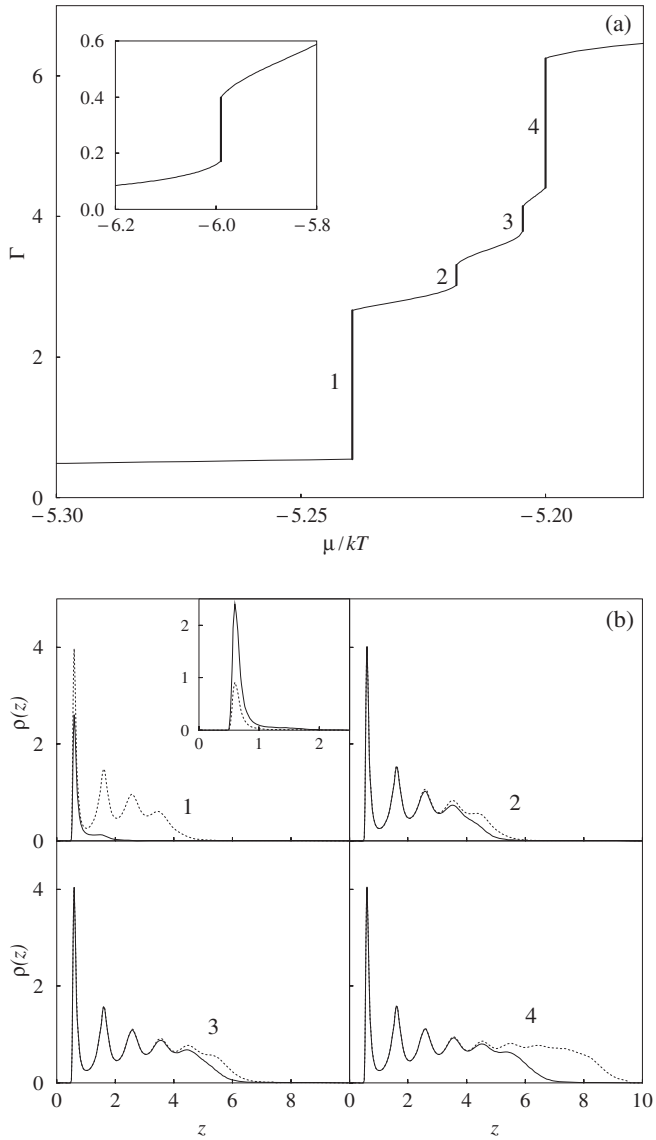


**Figure 3.** Adsorption isotherm (a) and the density profiles (b) for two coexisting phases. Numbers in both parts label consecutive adsorption steps. The calculations are for $H = 10$, $\varepsilon_1 = 9.5$, $\varepsilon_2 = 0.475$ and $T^* = 0.8$. The insets show the adsorption isotherms and the equilibrium density profiles for two coexisting phases, corresponding to the first, small branch of the phase diagrams in figure 2. The temperature is now $T^* = 0.73$.

HW. In this case the entire phase diagrams consist of branches depicting layering transitions. However, the shape of the branch corresponding to capillary condensation depends on the pore width. Obviously, the last feature is also observed for pores with identical walls.

Our calculations have demonstrated that the phase behaviour of the fluid confined in pores with differently adsorbing walls may be quite different from that observed in pores with identical walls and that even small changes in the adsorbing properties of one wall may lead

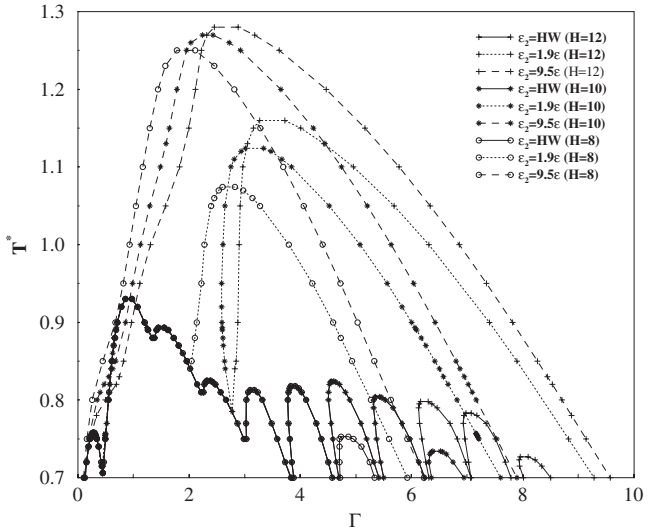


**Figure 4.** Influence of the pore width on the phase behaviour of a fluid confined to the pores with $\varepsilon_1 = 9.5$. The values of $\varepsilon_2$ and of $H$ are given in the figure.

to qualitative changes in the phase diagram. The results presented here remain in overall qualitative accordance with the results obtained for lattice systems using a Bragg–Williams approximation [14]. Obviously, the question arises whether the observed changes are not an artefact of a mean-field type approach. It is known that the theory applied by us 'amplifies' the tendency of the system to undergo layering transitions and enforces the first-order character of the transitions.

In the case of infinitely wide pores with identical walls, the surface phase diagram would reduce to the prewetting line, displayed in figure 1. Although we have not determined an exact value of the parameter $\varepsilon_1$ at which the first-order wetting at a single wall vanishes, we can state that for $\varepsilon_1 = 7.5$ the reduced wetting temperature equals approximately 1.03, whereas for $\varepsilon_1 = 4.75$ it becomes close to the bulk critical temperature. At still lower values of the adsorption energy the wall would be non-wet up to the bulk critical temperature. Thus, in the case of infinitely large pores formed between two differently adsorbing walls with $\varepsilon_2 \gtrsim 4.75$, the phase diagram would consist of two prewetting lines, each of them characterizing the wettability of a single wall. In the case of very weakly adsorbing second wall, the phase diagram for an infinitely wide pore would be just that shown in figure 1. However, the calculations performed for pores with widths $H = 8$, 10 and 12 were quite different to those for the $H = \infty$ phase behaviour. The presence of second weakly adsorbing ('dry') wall forces layerings causes the development of the wetting-like transitions. 'Dryness' of the second wall 'pushes' molecules towards the first wall and enforces their clustering and thus facilitates phase transitions. A question appears about the scenario of the changes in the phase diagram when the pore width increases to infinity. In particular it is of interest if there is a crossover between the phase behaviours shown in figures 1 and in 4 for any finite value of the pore width. Also, an important question that should be asked is whether the observed behaviour is not due to a mean-field approximation used in the density functional theory. These problems are now under study in our laboratory.

## Acknowledgment

This work was supported by the KBN under grant no 3 T09A 062 10.

## References

[1] Schön M 1993 *Computer Simulation of Condensed Phases in Complex Geometries (Lecture Notes in Physics)* (Berlin: Springer)
[2] Schoen M 2000 *Computational Methods in Surface and Colloid Science* ed M Borówko (New York: Marcel Dekker)
[3] Dietrich S 1999 *New Approaches to Problems in Liquid State Theory* ed C Caccamo *et al* (Amsterdam: Kluwer) pp 197–244
[4] Gelb L D, Gubbins K E, Radhakrisknan R and Sliwinska-Bartkowiak M 1999 *Rep. Prog. Phys.* **62** 1572
[5] Binder K and Luiten E 2001 *Phys. Rep.* **344** 179
[6] Müller M, Binder K and Albano E V 2000 *Physica* A **279** 188
[7] Ferrenberg A M, Landau D P and Binder K 1998 *Phys. Rev.* E **58** 3353
[8] Albano E V, Binder K and Paul W 2000 *J. Phys.: Condens. Matter* **12** 2701
[9] Müller K, Binder K and Albano E V 2001 *J. Mol. Liq.* **92** 41
[10] Müller M and Binder K 2001 *Phys. Rev.* E **6302** 1602
[11] Binder K, Müller M and Albano E V 2001 *Phys. Chem. Chem. Phys.* **3** 1160
[12] Carton E and Drzewiński A 1998 *Phys. Rev.* E **57** 2626
[13] Toxvaerd S and Stecki J 2001 *J. Chem. Phys.* **115** 1928
[14] Zagórski R and Sokołowski S 2001 *J. Colloid. Interface Sci.* **240** 219
[15] Zhou S 2000 *J. Chem. Phys.* **113** 8171
[16] Tarazona P 1985 *Phys. Rev.* A **31** 2672
Tarazona P 1985 *Phys. Rev.* A **32** 3148 (erratum)
[17] Weeks J D, Chandler D and Andresen H C 1971 *J. Chem. Phys.* **54** 5237
[18] Pizio O, Patrykiejew A and Sokołowski S 2000 *J. Chem. Phys.* **113** 10 761